JOURNAL OF AIRCRAFT
Vol. 32, No. 2, March–April 1995

CFD-Based Aerodynamic Approximation Concepts Optimization of a Two-Dimensional Scramjet Vehicle

Peter D. McQuade,* Scott Eberhardt,† and Eli Livne†
University of Washington, Seattle, Washington 98195

A direct numerical optimization methodology combining nonlinear programming and approximation concepts is studied in the context of CFD-based engine/airframe integration. It aims at reducing the number of full CFD analyses required in the course of an optimization, by replacing the original optimization problem by a set of approximate problems, thus reducing computational cost considerably. The performance of global local approximations (GLA) is tested and compared to that of a more common first-order Taylor series approximation. These approximations are obtained with alternative simplified aerodynamic analysis techniques corrected by CFD computations. A two-dimensional NASP-like configuration serves as a test case. In this article the basic procedure is reviewed and results based on optimization studies of the nozzle and forebody are presented. Problems associated with the application of GLA to CFD-based optimization are discussed and some solutions and insights are provided.

Nomenclature

a_{curve} = curvature parameter
c_∞ = freestream speed of sound
F = objective function
F_{net} = normalized net thrust (thrust − drag) (normalized by $\rho_\infty c_\infty^2$)
f_a = behavior function for approximate analysis
f_d = behavior function for detailed analysis
G = design constraints
h_n = nozzle height, m
L_{cowl} = cowl length, m
L_{fb} = forebody length, m
L_{ramp} = ramp length, m
L_{ref} = reference length, m
X = design variables
α = nozzle turning angle, deg
β = correction factors for GLA
γ = ratio of specific heats
θ_{nose} = nose angle, deg
θ_{ramp} = ramp angle, deg
ρ_∞ = freestream density

Introduction

INCREASING computing power and improvements in computational algorithms in the last two decades have made CFD into an effective tool for the understanding of basic flow phenomena as well as for the analysis of internal and external flows in real, complex aerospace vehicles. CFD has already contributed to the development of several aerospace vehicles and their propulsion systems. In particular, preliminary analysis of National Aerospace Plane (NASP) concepts has relied heavily on CFD. With the growing confidence in the reliability of computational predictions, it becomes natural to turn to automated synthesis with CFD, and several approaches to the problem can be identified in the literature.[1,2]

CFD-based automated synthesis presents many challenges. The computational cost associated with the CFD analysis of realistic configurations is usually large. In automated synthesis, where a configuration is systematically changed to improve some performance criteria, and to meet some constraints (a process that requires many repeated analyses), the computational cost can become prohibitive. But computational cost is not the only difficulty in automated synthesis using CFD. Selection of design variables must be done carefully and any discontinuities introduced by the solution technique (such as rapidly changing grid lines or algorithm switches) should be carefully treated. Also, the presence of shock waves and other discontinuities in the solution may cause difficulties with gradient-based optimization algorithms. And, if the design process is to be automated, efficient and reliable computations of design sensitivities are important in order to point a gradient-based search algorithm in the correct direction. Techniques for obtaining analytical derivatives of CFD analysis results with respect to design variables have been reported in the last three years.[3–5]

It has long been recognized, in the context of structural synthesis, that computational analysis carried out for the purpose of automated design should not necessarily be subject to the same requirements and criteria, such as accuracy or convergence, as in the case of detailed single analysis.[6] For a NASP-like vehicle, an approximate technique, such as the Newtonian flow theory, may be used during initial analyses, and gradually phased out and replaced by CFD as the design process converges to an optimum.

Combining nonlinear programming with approximation concepts (NLP/AC) has proven to be successful in solving structural optimization problems.[7,8] NLP is general. No a priori knowledge of the active constraints that drive a certain design is needed. In multidisciplinary optimization this is especially important, since optimality criteria developed from within each individual discipline may be found to be misleading in the integrated multidisciplinary problem.

The main idea behind approximation concepts[9] is to replace the original problem by an approximate problem and apply the optimizer (any NLP algorithm for constrained minimization) only to the approximate problem. A sequence of such approximate optimization problems is then solved until convergence to a locally optimal solution is obtained. Thus, only a small number of detailed analyses are carried out during optimization, whereas the many function evaluations needed by the optimizer are based on approximations that are computationally cheap.

A detailed, high-fidelity, analysis model and its associated sensitivity analysis can be used as the basis of the approximate

Received Aug. 31, 1992; revision received Feb. 17, 1994; accepted for publication Feb. 17, 1994.

*Graduate Student, Department of Aeronautics and Astronautics.
†Assistant Professor, Department of Aeronautics and Astronautics. Member AIAA.

problem, or to modify it. This is an iterative process, with the approximate model being improved after each complete optimization ("cycle") using the approximate model. The simplest such approximation is a first-order Taylor series representation of the desired properties.[8] The coefficients in the series are found from the detailed analysis and the sensitivity analysis. Results of exploratory experimentation with NLP-based CFD/Taylor series optimization of aerodynamic configurations have been reported in Refs. 3–5.

The Taylor series approach, however, is only guaranteed to be accurate in the immediate vicinity of the baseline design. A method of introducing more global accuracy has been recently introduced by Haftka.[10–12] Denoted GLA, the method integrates two levels of analysis techniques as follows. A detailed, high-fidelity, analysis is used a small number of times along the design synthesis path. The results of these analyses are used to fine-tune the simplified, computationally cheap, analysis techniques, which are used by the optimizer. Thus, the full optimization problem is solved as a sequence of approximate optimization problems. The approximations, however, are now based on models that can capture more of the basic physics, and nonlinear behavior, of the problem at hand than can be captured by Taylor series approximations.

It is the purpose of this research to examine global-local approximations for CFD-based optimization applied to a two-dimensional scramjet-powered vehicle. This problem captures many of the significant features and difficulties with CFD-based optimization. As such, it serves as a valuable test case leading to important lessons and insights on the way to optimization techniques capable of addressing more complex engine-airframe integration configurations. Some experimental results are available for this problem, and it was already used for other studies in CFD-based optimization.[4]

This article opens with a short discussion of the test problem chosen. This is followed by a discussion of how global-local approximations are formed. Some algorithmic modifications needed for automated aerodynamic design using CFD, and GLAs are then presented. Three simplified aerodynamic models are employed in the GLAs. These models are outlined next. The accuracy of the resulting GLAs is compared to that of the first-order Taylor series approximations by means of single-variable parametric studies for the nozzle/afterbody region. Design optimization results with the different approximation techniques are used to demonstrate the viability of global-local approximations in CFD.

Design Problem

A complete two-dimensional scramjet vehicle configuration is to be designed and is shown in Fig. 1. The normalized net thrust (thrust-drag) is selected as the objective function. Geometric design variables define the front end and nozzle of the vehicle. In this study, the nozzle ramp wall geometry is limited to a family of skewed parabolas as shown in Fig. 2. The geometry is characterized by the initial wall angle α, and the quadratic coefficient a_{curve}. Note that in this study alternative design variables are used that can lead to better optimization results. Design variables for the front end are lengths of the nose and ramp, the vertical locations of their corners, and the fore-aft position of the cowl lip (Fig. 3).

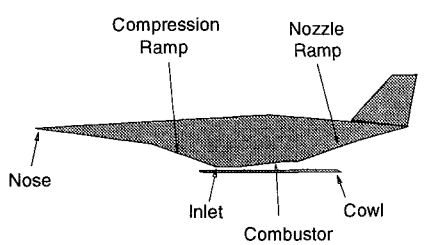

Fig. 1 Two-dimensional scramjet vehicle.

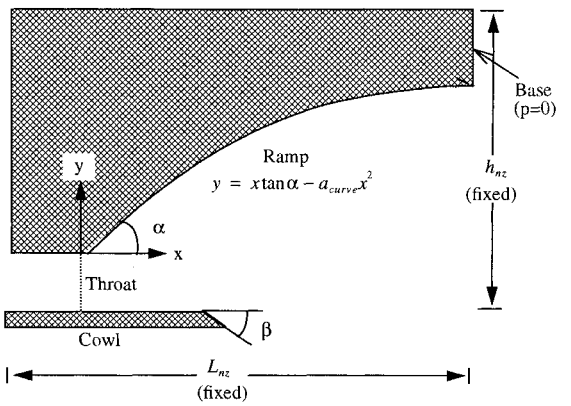

Fig. 2 Geometry of the nozzle.

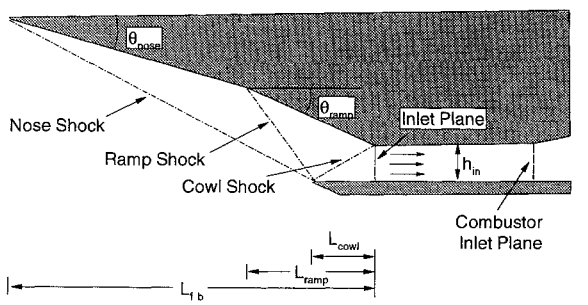

Fig. 3 Geometry of the front end.

The only constraints on the design are side constraints on vehicle dimensions. The following side constraints are imposed: the initial ramp angle α must be between 10–26 deg; the nozzle exit plane height has to be between 4–6.5815 m (which was the forebody height). No direct constraints are placed on the curvature parameter a_{curve}. For the front end the nose and ramp angles are bounded as follows: 6.0 deg $\leq \theta_{nose} \leq$ 11.0 deg and 11.5 deg $\leq \theta_{ramp} \leq$ 20.0 deg. The height at the combustor inlet is fixed at 0.6667 m.

Since the wall flow in the nozzle region is essentially isentropic, the investigation focuses first on the synthesis of the nozzle only. This avoids the issue of the effect of discontinuities (shocks) on the approximation concepts, and thus serves to demonstrate the potential of GLAs. In this case the forebody, compression ramp, and combustor inlet properties are held constant at values that were found in a separate optimization of those parts of the vehicle. The contribution of drag due to base pressure is allowed to vary as the nozzle geometry changes. If the height of the nozzle is less than the height of the forebody, then the pressure on the bluff base is set to zero. The nozzle height is not allowed to be greater than the forebody height for the nozzle optimizations, and the nozzle length is fixed.

The techniques are then applied to optimization of the forebody/inlet region. To investigate the behavior of GLAs in a reasonably general type of flow regime, the problem is not limited to "perfect" shock placement, with the nose and ramp shocks impinging on the cowl lip and the resulting reflection hitting the corner of the ramp. That is, arbitrary shock configurations are allowed, and so there is the possibility of shock impingements on wall surfaces, and shocks passing directly into the inlet. This poses a much more challenging test of GLAs than when applied to the nozzle optimizations.

Optimization Technique

Designating the objective function F, the vector of design variables $\boldsymbol{X}$, and the vector of behavior constraint functions $\boldsymbol{G}$, the design optimization problem is a nonlinear programming problem in the form

$$\max \ldots F(\boldsymbol{X}) \tag{1}$$

subject to

$$G(X) \leq 0 \tag{2}$$

and the following side constraints:

$$X^L \leq X \leq X^U \tag{3}$$

Tools

The modified method of feasible directions[13] as implemented in design optimization tools (DOT)[14] is used for the numerical solution of the constrained optimization problem. Derivatives of objective and constraint functions with respect to design variables are obtained using finite differences. Analytic sensitivities offer major advantages and can be used[4] to save computational resources and prevent numerical difficulties associated with step-size selection. They are, however, algorithm-dependent and can be difficult to obtain. The finite difference approach is simple to incorporate, and thus chosen for this study that focuses on other aspects of the optimization process.

Applying GLAs

To achieve an optimum design many function evaluations of $F(X)$ are required. Each function evaluation, using CFD as the only tool, requires a complete CFD solution. Even under the most ideal circumstances this is too expensive to consider as a practical design tool.

In order to reduce the number of CFD analyses required, optimization is based on the approximation concepts approach.[7] Information from the CFD analysis at a baseline design is used to construct approximations of the objective and constraint functions, which are cheaper computationally. The actual problem is then replaced by a series of approximate problems in which the optimizer interacts with the approximate analyses in its search for an optimum. As the design moves away from the baseline, the accuracy of the approximations deteriorates. To protect the accuracy, move limits are imposed on the design variables to prevent them from moving too far from the baseline during any one cycle. An optimization cycle is a complete optimization using only the approximate problem.

In the application of GLAs to this problem, simplified aerodynamic analysis techniques are used to determine approximate solution behavior. The GLA can be applied to either point properties (such as wall pressures and inlet plane flow properties), or to integral properties (such as net thrust). If the objective function is itself an integral property, the use of point properties in the GLA can often capture nonlinear objective function behavior that use of the integral property cannot.

Let $f(X)$ be some behavior function of the design variables, e.g., wall pressure at some point. Let $\beta(X)$ be a correction factor used to correct the result of an approximate analysis, $f_a(X)$, to match the result of the more detailed (CFD) analysis, $f_d(X)$; i.e.,

$$\beta(X) = [f_d(X)/f_a(X)] \tag{4}$$

$\beta(X)$ is evaluated at the baseline design X^0, and then extrapolated to other design points X by a first-order Taylor series

$$\beta(X) = [f_d(X)/f_a(X)] \approx \beta(X^0) + [\nabla\beta(X^0)]^T \Delta X \tag{5}$$

Differentiation of the expression for $\beta(X)$ with respect to the design variables leads to an expression of the gradient of β in terms of the gradients of the approximate and detailed analyses as follows:

$$\nabla\beta(X^0) = \nabla \frac{f_d(X)}{f_a(X)}\bigg|_0 = \beta(X^0)\left(\frac{1}{f_d}\nabla f_d - \frac{1}{f_a}\nabla f_a\right)\bigg|_0 \tag{6}$$

The CFD analysis and gradient computations are carried out at the baseline design point. The same is done with the approximate computations, and the correction factor equations are established for all relevant behavior functions (i.e., for all wall and inlet plane points). From that moment on, the optimizer calls the approximate analysis only and it, in turn, is corrected by the variable correction factor (5).

With the completion of an iteration, a new baseline design is determined. Detailed analysis and gradient calculations are carried out at that point, and the process is repeated until convergence is reached.

Aerodynamic Analysis Techniques

Aerodynamic analysis models are used for the forebody and nozzle flows of the vehicle. For the nozzle design two approximate analysis techniques are used in conjunction with the CFD analysis. The most sophisticated is a simple two-dimensional steady method of characteristics (MOC) model.[15] A pseudo-one-dimensional isentropic flow analysis is the second.[15] For the front end of the engine, where the flow is dominated by strong shocks, an approximate model based on oblique shock relations is developed and tailored to model several different possible shock structures.

For comparison purposes, a local approximation is used based on a first-order Taylor series representation of wall pressures and inlet plane flow properties in terms of the design variables.

The CFD code used in this study is the Steger-Warming, implicit time-marching algorithm for solving the unsteady Euler equations to a steady state.[16] The scheme uses flux-vector splitting and upwind differences, and is second-order accurate spatially everywhere but in the vicinity of large pressure gradients. At these points, typically shock waves, the algorithm drops to first-order to capture the flow features without spurious oscillations. The code is written in generalized curvilinear coordinates for a structured mesh system.

At each optimization cycle a new finite-difference mesh must be generated for the new geometry. Flow solutions can be greatly affected by the quality of the grid. The grid generation problem is a key element in making an optimization run possible. An inappropriate grid might result in grid-dependent pressure spikes or diffusion in the solution. As the shape of the vehicle is changed during optimization, new grids must be generated in a way that will eliminate such problems. A hybrid elliptic/algebraic grid generator was created that balances grid quality with low computational cost.

A typical nose-to-tail grid is shown in Fig. 4. Since the vehicle cowl is not connected to the vehicle in the two-dimensional simulation, a zonal grid is used. The cowl is actually defined by two consecutive grid lines, one representing the upper surface and the second, the lower.

The CFD code was run in two parts. The forebody/inlet region is treated first. The resulting combustor inlet flow is averaged across the inlet plane and used to form the upstream boundary conditions for the one-dimensional constant Mach number combustor model, which is run separately. The re-

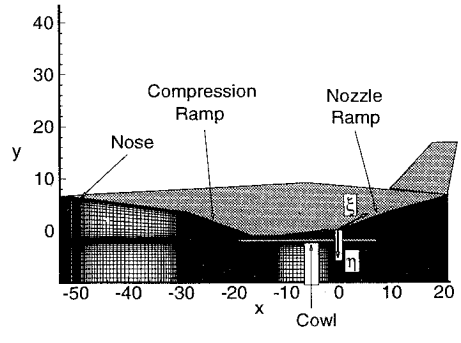

Fig. 4 Finite difference mesh for CFD code.

sulting combustor outlet flow properties and the external flow solution form the upstream boundary conditions for the nozzle/afterbody CFD model. Since the forebody/inlet region is held fixed during the course of a nozzle/afterbody optimization it does not have to be solved with each new nozzle/afterbody geometry.

Experimental results for a nozzle/afterbody are quoted in Ref. 4 and are used here for validation. Figure 5 is a comparison of the pressure distribution along the nozzle ramp for the CFD code and the experimental results.

For the GLA the MOC is selected as a quick, yet fairly accurate, analysis technique. A rigorous application of the MOC to our case can theoretically reproduce the results of the Euler solver, but to simplify the problem, several simplifications were made. First, the interaction of the characteristics with the shock wave(s) emanating from the cowl lip is neglected. In addition, all characteristics used are considered to originate from the two expansion corners shown in Fig. 6. Therefore, there is a region immediately downstream of the ramp corner where no characteristics impinge on the wall, and thus the curvature of the wall is not accounted for. In actual fact, the MOC model could be improved to fit shock waves and capture all of the salient features of the flow, but this is not as conducive to generality as the CFD code is. A typical solution of the nozzle using MOC is shown in Fig. 6.

Next, a one-dimensional, isentropic flow analysis technique is used that illustrates best the dependence of a global approximation on a correction by the detailed CFD analysis. With the one-dimensional analysis no multidimensional features of the flow can be captured. The flow is assumed to be shock-free and to expand isentropically. An immediate difficulty is the lack of a boundary on one side of the nozzle. Thus, one-dimensional flow analysis, at first, seems impossible. To handle this problem the CFD solution is used to locate the plume boundary, or contact surface, between the streams from either side of the cowl, i.e., from the combustor and the external flow. This contact surface is then used as the "other boundary." Each time the CFD solver is called a new contact surface is found and used in the following one-dimensional analyses. Clearly, as the optimizer searches further from the initial baseline solution the one-dimensional analysis will begin to lose accuracy, partly because the actual contact surface changes. Move limits on the design variables, as described previously, help protect the one-dimensional simplified analysis against loss of accuracy.

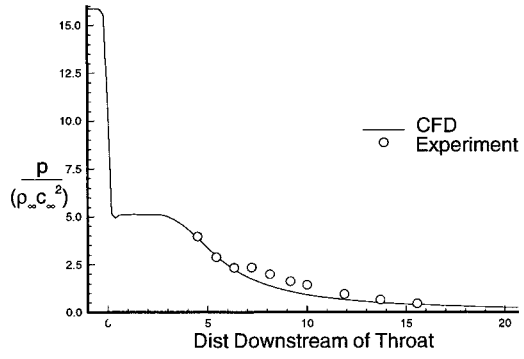

Fig. 5 Comparison with experiment.

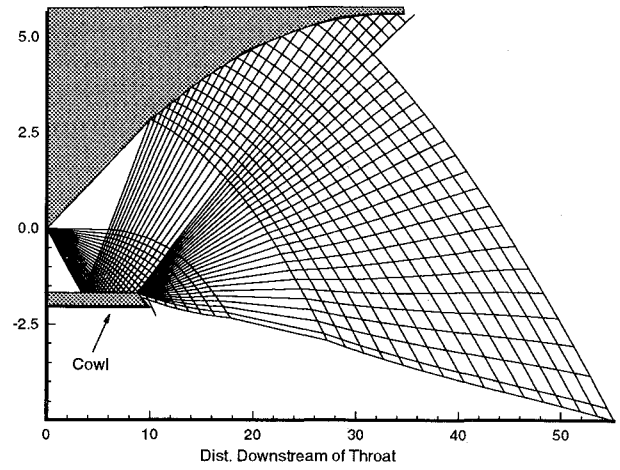

Fig. 6 MOC solution of nozzle.

It should be noticed that there is a hierarchy in accuracy and complexity of the three analysis methods used for the nozzle. The CFD method is most accurate, but also most demanding computationally. The one-dimensional analysis method is very simplified and the least accurate. But its coding and computational cost is extremely low, leading to major gains in computational efficiency when used in the optimization process.

The simplified analysis for the forebody calculations is based on simple oblique-shock theory. In order to examine the behavior of the approximation concepts in a relatively complicated, nonisentropic flow regime, forebody and inlet shock placements, which differ from the well-accepted "perfect" shock placements, are allowed. Then the simplified analysis is required to take into account major shock/wall, shock/shock, and shock/shear-layer interactions for a large number of alternative shock structures depending on the forebody geometry. It neglects some shock reflections and interactions in order to make it as simple as possible. In addition, the approximate model treats the flow only up to the expansion corner at the end of the ramp. Thus, it does not model the often-complicated flow inside the inlet duct, which the CFD model does capture. Nevertheless, in the course of the optimizations, it is found that this approximate model does duplicate quite well the general behavior of net thrust with respect to the design variables that is found by the CFD model.

Combustor Model

Only a simple model is used for the combustor. It is fully coupled with the forebody and nozzle flows. The combustor is modeled as a one-dimensional, constant-Mach number process. The fuel-air mixture is assumed to be a perfect gas with $\gamma = 1.4$. The addition of mass due to fuel injection is neglected. Although it would be more customary to employ a constant-pressure combustor, it is pointed out in Ref. 17 that the constant-Mach number combustor offers two advantages from an analysis standpoint. It explicitly avoids choking in the combustor, and it greatly simplifies the analysis. Such a combustor would be difficult to employ in practice, as it would require that the heat addition be specifically tailored along the length of the combustor. However, for the purposes of demonstrating different optimization strategies for the coupled propulsion/aerodynamic synthesis of the scramjet vehicle, the constant-Mach number combustor provides a useful, simple tool that captures the salient features of total temperature increase and total pressure decrease.

The geometry of the combustor is held fixed. However, changes in the inlet design impact the flow through the combustor, creating different inlet conditions for the nozzle. Thus, for inlet optimizations, full-vehicle calculations are required. Note that the area expansion in the combustor results in a large portion of the thrust coming from the combustor. In this study the, "combustor thrust" accounted for roughly 50% of the total thrust.

Nozzle Results

The CFD-based GLAs were first applied to the optimization of the nozzle/afterbody, holding the combustor conditions and front end fixed. Specified throat and freestream conditions were used. The inflow conditions for the external flow were set equal to the freestream values. The various

Table 1 Results of nozzle optimizations

Method	α	a_{curve}	F_{net}[a]	CFD calls	Cost per analysis
Initial design	18.000	0.0050	18.05	—	—
CFD	20.541	0.0032	19.71	22	1.0
One-dimensional	26.000	0.0082	18.42	—	—
MOC	26.000	0.0082	18.42	—	—
Taylor	20.362	0.0031	19.71	7	0.0098
One-dimensional GLA	20.850	0.0035	19.71	7	0.0083
MOC GLA	20.563	0.0033	19.70	7	0.0109

[a]For all cases shown, F_{net} is calculated using CFD.

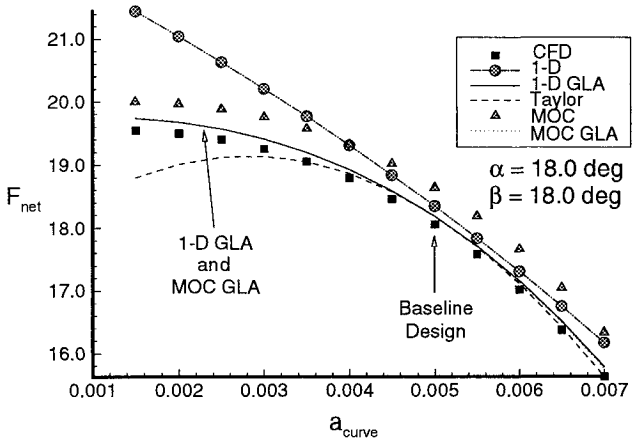

Fig. 7 Parametric study of normalized thrust vs nozzle ramp curvature coefficient.

optimization approaches, based on CFD alone, Taylor series, one-dimensional GLA and MOC GLA were compared for solution quality and computational efficiency. The "all CFD" optimization results were the baseline against which all other methods were compared.

Parametric Studies

Parametric studies using the various approximation techniques were first conducted and a typical example is shown in Fig. 7. This figure shows the normalized net thrust variation with nozzle ramp curvature coefficient a_{curve}. The baseline design is also shown in the figure. In addition to the CFD, Taylor series, and GLA results, the uncorrected one-dimensional and MOC results are also shown. The importance of scaling the approximate analysis techniques by the CFD results is evident. The success of these global approximation methods in capturing the nonlinearity of the problem is also evident. The first-order Taylor series using direct design variables[8] cannot capture this nonlinearity as well, although it provides decent accuracy near the base design point. GLA results are based on wall pressures fine-tuned by the CFD calculations.

Nozzle Optimization

For each of the nozzle-only optimizations, the design was optimized using the initial ramp angle α, and the nozzle exit height h_{nz}, as design variables. Optimizations were carried out for all analysis models and approximation techniques. The resulting designs were compared and the savings in computer resources for each method were then found. The figure of merit for these savings was the number of required calls to the CFD solver for analysis purposes, exclusive of the calls used to calculate the gradients of the objective function and constraints.

For all these optimizations, the initial values of α and h_{nz} were 18.0 deg and 3.74 times the combustor exit height, respectively. This corresponds to an a_{curve} of 0.005. Move limits of 10% were used for the GLAs and Taylor series.

The results for all the nozzle optimizations are given in Table 1. Shown are the optimum designs (in terms of α and a_{curve}), the normalized net thrust, and the required number of calls to the CFD solver. For consistency of comparison, the optimum net thrust values were found by applying the CFD solver to the optimum design found by each method. Also shown is the cost in computer time for one approximate analysis in an optimization cycle for each approximation concept, normalized by the cost for one analysis using CFD only.

The table shows that the CFD-only optimization required 22 calls to the CFD solver (exclusive of calls for calculating gradients). Each of these calls required 66 min of CPU time on an IBM RS 6000 workstation.

The uncorrected one-dimensional and MOC optimum designs were very different from the CFD optimum. They both optimized to the same design, because each hit the maximum allowable α and then set the base area nearly to zero by adjusting h_{nz}. Their optimum values of F_{net} are 6% lower than for the CFD, Taylor series, and GLA methods.

The Taylor series and the MOC GLA optimized to designs very close to that which the CFD-only optimization selected, but did so with only seven calls to the CFD solver, respectively. This represents a savings in computer time of 68%. Although 10% move limits were imposed on the design variables for these optimizations, it is possible that greater move limits could be imposed, perhaps resulting in some further savings. Although the one-dimensional GLA optimum design is not quite as close to the CFD optimum design, the optimum net thrust is almost identical, and the savings in CFD calls are the same as for the Taylor series and MOC GLA.

The relative cost of one analysis within a given cycle was about 24% cheaper for the one-dimensional GLA than for the MOC GLA. It was about 15% cheaper for the one-dimensional GLA than for the Taylor series. Each of these methods required about the same number of analyses within each optimization cycle (about 14). Thus, the one-dimensional GLA solution is the most cost-effective of the approximation concepts tested in the nozzle region.

Figure 8 shows the nozzle geometry, including the computational mesh, for the initial and final (optimized) designs. Note how the final solution has eliminated the base area that is a major source of drag.

Optimization histories for the CFD-only, Taylor series, and the GLAs are shown in Figs. 9–11. The effectiveness of the Taylor series and the GLAs are highlighted by Fig. 9, which portrays F_{net} vs CFD calls. Recall that each CFD analysis for the GLA optimizations corresponds to one optimization cycle in which there will be about 14 calls to the approximate analyses. In the case of the CFD-only optimization, all calls for analysis result in additional CFD calculations. Figures 10 and 11 depict the histories of the design variables α and a_{curve}, respectively. Note that the Taylor series and one-dimensional GLA curves are relatively smooth up to the final design, whereas the MOC GLA histories are rather jagged. However, all these methods find nearly the same optimum design.

Pressures along the walls are used here as the behavior functions to be approximated. These approximate pressures are then integrated to obtain thrust, drag, and net thrust.

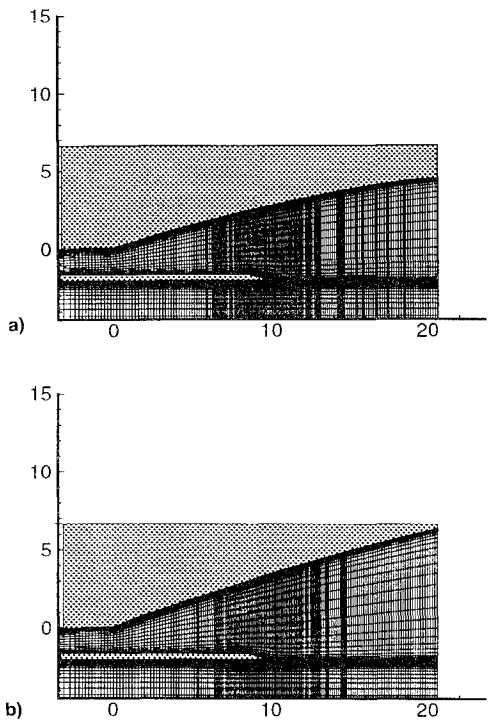

Fig. 8 Nozzle design: a) initial and b) final design.

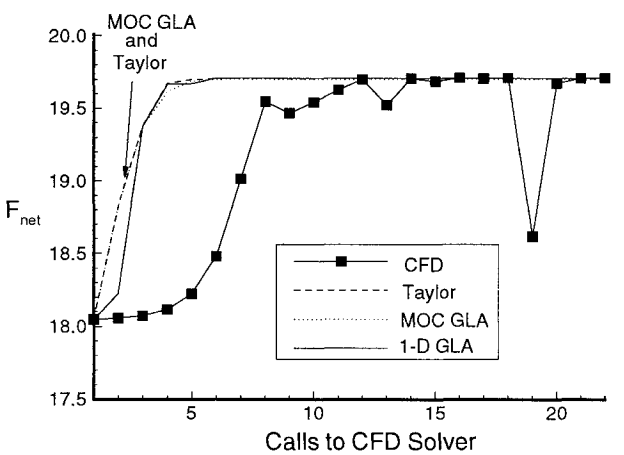

Fig. 9 Optimization history of F for the nozzle.

Correcting the pressures by CFD values presents a problem when two grid systems move and change with respect to each other, such as in the case of CFD and MOC. Here, a reference, fixed grid is used for applying the correction factors. This fixed grid contains a constant number of points at normalized stations. The CFD and MOC grids have a variable number of points. Pressures from each grid are interpolated and transferred to the same points on the reference grid where corrections are applied.

Forebody Results

The success of GLAs in the nozzle optimization studies is encouraging. Still, the application of GLAs to CFD-based design faces many difficulties. Serious problems arise when, due to changes in design variables, the topology of the flowfield is changing. Shock waves and shear layers as well as separation lines may move. Devising simplified analysis techniques for these situations is challenging. Correcting these simplified analyses with the Taylor series or GLA method is also problematic and can be algorithm-dependent. When CFD algorithms that "smear" shock waves are used to correct the results from approximate analyses based on ideal shocks, the correction factor scaling itself may be questionable even if the

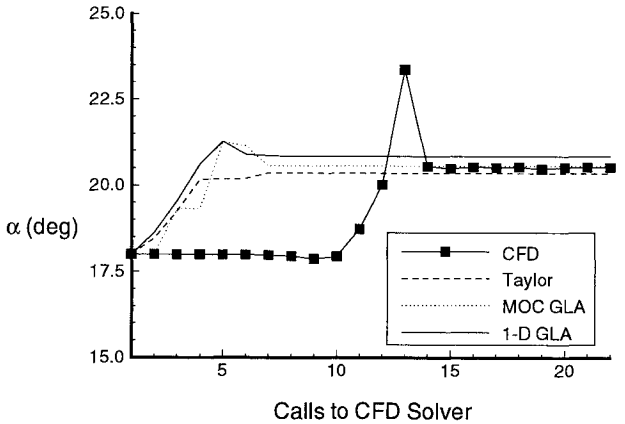

Fig. 10 Optimization history of α.

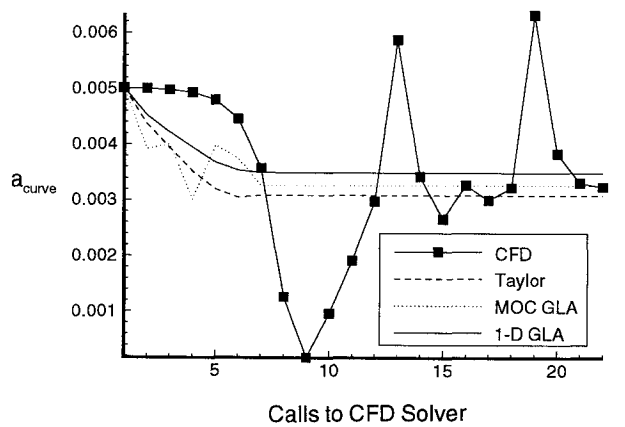

Fig. 11 Optimization history of a_{curve}.

approximate analysis alone compares favorably with the overall CFD results. Gradient computations in the presence of moving shocks can also be difficult.

Optimization of the front end of the vehicle is attempted next in an effort to study the GLA in a flowfield controlled by strong shocks. Although only design variables associated with the front end are varied, the flow analysis is carried out for the whole vehicle. This is because the combustor and nozzle flows as well as the forebody flow react to changes in the design variables. All forebody optimizations were started with an initial design that corresponds to a nose angle of 8.0 deg, a compression ramp angle of 18.0 deg, and a cowl lip position of 3.2 m relative to the inlet corner.

The optimizations performed solely with CFD analyses led to the design shown in Table 2. Twenty-five calls to the CFD solver were required (exclusive of those for gradient calculations). A history of this optimization is shown in Figs. 12 and 13. The approximate method alone (using the oblique shock theory model for the front end and the method of characteristics for the nozzle) also optimized to a design close to this one, as shown.

Point properties (wall pressures and inlet flow properties) are used as behavior functions, as with the nozzle optimizations. However, the attempt to use point pressures for corrections by GLA on the forebody was not successful. In fact, the behavior of F_{net} within any given cycle was extremely erratic. This was found to be due, in large part, to the movement of shock impingement points during the calculation of $\nabla\beta(X^0)$. Such movement cannot be captured by the gradient calculations as they are implemented, which leads to incorrect gradient calculations, and thus results in erroneous correction factors. In addition, the CFD and approximate methods do not capture shocks equally crisply, which may lead to further error in the correction factors. Thus, a complete optimization using the point property GLA could not be performed.

Table 2 Forebody optimization results

Method	Θ_{nose}	Θ_{ramp}	L_{ff}	L_{ramp}	L_{cowl}	F_{net}[a]	CFD calls
Initial design	8.000	18.000	35.000	13.000	3.200	5.422	——
CFD	7.294	19.998	34.899	12.869	3.613	18.869	25
Approximate	7.705	19.998	34.940	12.932	3.393	17.316	——
Taylor	7.045	20.063	26.977	8.541	2.794	9.214	7
Integral GLA (zeroth order)	7.786	20.027	35.149	13.184	3.491	18.613	1

[a]For all cases shown, F_{net} is calculated using CFD.

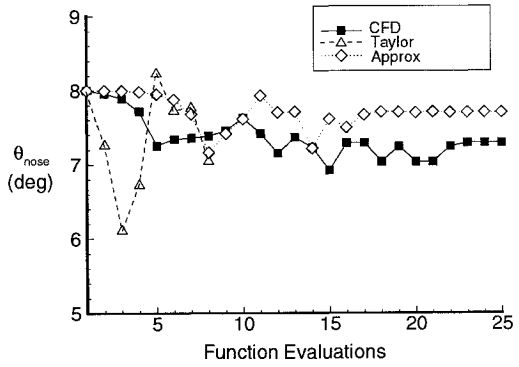

Fig. 12 Optimization history of θ_{nose} for the forebody.

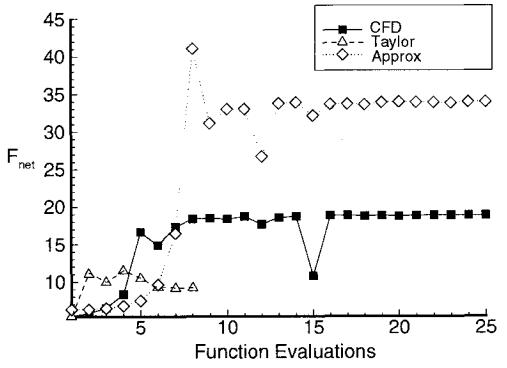

Fig. 13 Optimization history of F for the forebody.

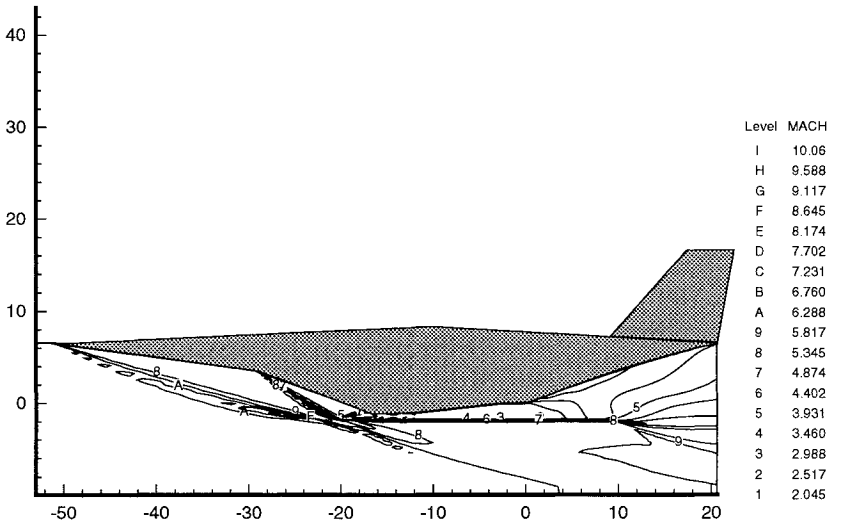

Fig. 14 Optimized vehicle design.

The Taylor series approach suffers this same response to shock movement during gradient calculations, but to a much smaller degree. Thus, Taylor series optimization results are presented. Note that, although the Taylor series yields optimum values of Θ_{nose} and Θ_{ramp}, which are quite close to those found by the CFD optimizations, the lengths are substantially in error.

Instead of correcting local properties such as wall pressures, the GLA was then applied to the integrated properties: thrust, drag, and net thrust. Since the use of derivative information in the correction factor calculations was still problematic, the GLA was applied to the integral properties, but with only zeroth-order scaling [no gradient information in Eq. (5)]. This method then optimized to the same design as the CFD and the approximate method.

In Fig. 14 a complete vehicle solution is shown. We include this figure to show the CFD solution with the optimum geometry found in the two optimizations. A complete optimization, involving design variables for the forebody and nozzle/afterbody changing simultaneously, is beyond the scope of this article. Additional information regarding problems with shocks in the forebody can be found in Ref. 18.

Conclusions

An exploratory study of the application of GLAs using approximation concepts and CFD was carried out for an integrated propulsion/aerodynamic synthesis of a scramjet vehicle.

The two-dimensional scramjet design case captures many inherent difficulties associated with the application of GLA concepts to optimization with CFD. Their application is found to be successful in the nozzle case, a problem with a simple, nearly isentropic wall flow, but not in the front end design problem, which had moving shock impingement points.

Difficulties with GLA in this case were found to be caused by discontinuities in the flowfield and the sensitivity of pressure distribution corrections to such discontinuities. The use of integral measures as behavior functions to be corrected improved the results. The identified problems associated with modeling flow discontinuities and changing grids present a challenge for GLA and call for further research.

References

[1]Tolson, R. H., and Sobieszczanski-Sobieski, J., "Multidisciplinary Analysis and Synthesis: Needs and Opportunities," AIAA Paper 85-0584, 1985.

[2]"Computational Methods for Aerodynamic Design (Inverse) and Optimization," Specialists' Meeting of the Fluid Dynamic Panel, Loen, Norway, May 1989, AGARD CP-463, 1990.

[3]Frank, P. D., and Shubin, G. R., "A Comparison of Optimization-Based Approaches for Solving the Aerodynamic Design Problem," Third Air Force/NASA Symposium on Recent Advances in Multidisciplinary Analysis and Optimization, San Francisco, CA, Sept. 1990.

[4]Baysal, O., and Eleshaky, M. E., "Aerodynamic Design Optimization Using Sensitivity Analysis and Computational Fluid Dynamics," *AIAA Journal*, Vol. 30, No. 3, 1992, pp. 718–725.

[5]Levine, M., Ide, H., and Hollowell, S., "Multidisciplinary Hypersonic Configuration Optimization," Third Air Force/NASA Symposium on Recent Advances in Multidisciplinary Analysis and Optimization, San Francisco, CA, Sept. 1990.

[6]Schmit, L. A., "Structural Analysis—Precursor and Catalyst," *Recent Experiences in Multidisciplinary Analysis and Optimization*, Pt. 1, 1984, pp. 1–17 (NASA CP-2327).

[7]Schmit, L. A., "Structural Optimization—Some Key Ideas and Insights," *New Directions in Optimum Structural Design*, edited by E. Atrek, R. H. Gallagher, K. M. Ragsdell, and O. C. Zienkiewicz, Wiley, New York, 1984.

[8]Haftka, R. T., and Gurdal, Z., *Elements of Structural Optimization*, 3rd ed., Kluwer Academic Publishers, Dordrecht, The Netherlands, 1992.

[9]Barthelemy, J.-F. M., and Haftka, R. T., "Recent Advances in Approximation Concepts for Optimum Structural Design," NASA TM-104032, March 1991.

[10]Haftka, R. T., "Combining Global and Local Approximations," *AIAA Journal*, Vol. 29, No. 9, 1991, pp. 1523–1525.

[11]Chang, K. J., Haftka, R. T., Giles, G. L., and Kao, P.-J., "Sensitivity-Based Scaling for Correlating Structural Response from Different Analytical Models," AIAA Paper 91-0925, April 1991.

[12]Hutchison, M., Unger, E., Mason, W., Grossman, B., and Haftka, R., "Variable-Complexity Aerodynamic Optimization of an HSCT Wing Using Structural Wing-Weight Equations," AIAA Paper 92-0212, Jan. 1992.

[13]Vanderplaats, G. N., *Numerical Optimization Techniques for Engineering Design: With Applications*, McGraw-Hill, New York, 1984.

[14]Vanderplaats, G. N., and Hansen, S. R., *DOT Users' Manual*, Vanderplaats, Miura & Associates, Goleta, CA, 1990.

[15]Liepmann, H. W., and Roshko, A., *Elements of Gasdynamics*, Wiley, New York, 1957.

[16]Steger, J. L., and Warming, R. F., "Flux Vector Splitting of the Inviscid Gasdynamic Equations with Application to Finite Difference Methods," NASA TM-78605, July 1978.

[17]Armangaud, F., Decher, R., Koopman, A., and Lafosse, B., "One-Dimensional Modeling of Hypersonic Flight Propulsion Engines," AIAA Paper 89-2026, July 1989.

[18]McQuade, P. D., "CFD-Based Approximation Concepts for Aerodynamic Design Optimization with Application to a 2D Scramjet Vehicle," Ph.D. Dissertation, Dept. of Aeronautics and Astronautics, Univ. of Washington, Seattle, WA, Aug. 1992.